



# Panchromatic and Multispectral Image Fusion via Alternating Reverse Filtering Network

NeurIPS-2022 Conference

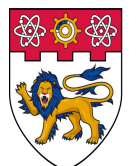
**Keyu Yan<sup>1,2</sup>, Man Zhou<sup>1,2</sup>, Jie Huang<sup>2</sup>, Chengjun Xie<sup>1</sup>, Feng Zhao<sup>2</sup>, Chongyi Li<sup>3</sup>, Danfeng Hong<sup>4</sup>**

<sup>1</sup>**Hefei Institute of Physical Science, Chinese Academy of Sciences**

<sup>2</sup>**University of Science and Technology of China**

<sup>3</sup>**Nanyang Technological University, Singapore**

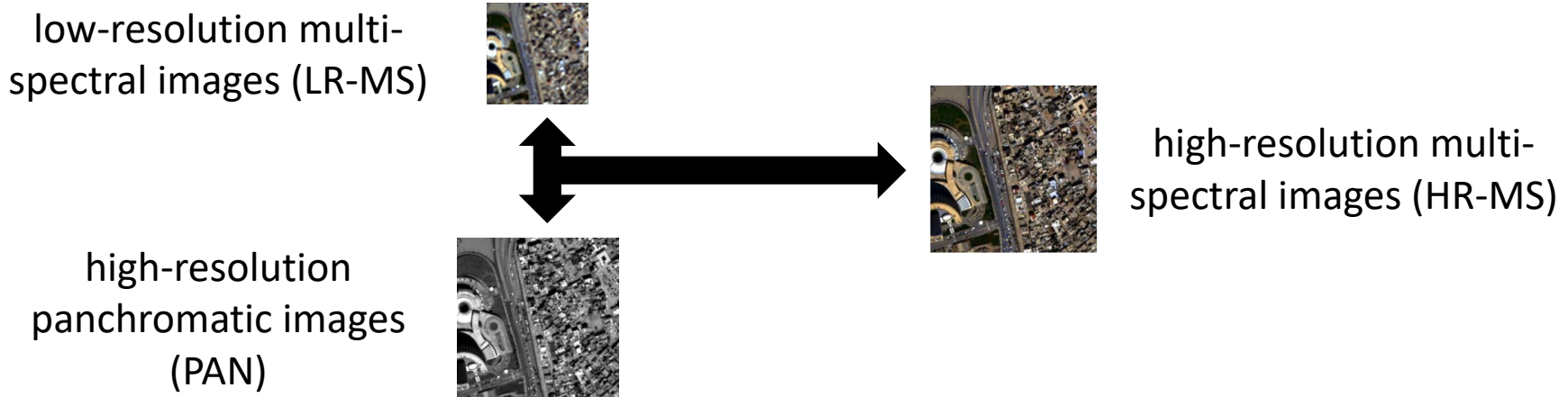
<sup>4</sup>**Aerospace Information Research Institute, Chinese Academy of Sciences**



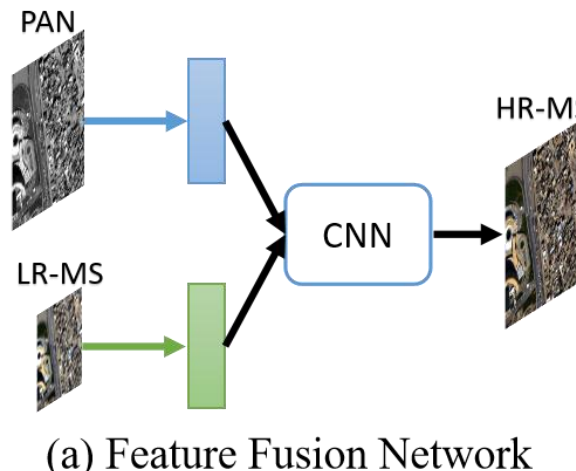
**NANYANG  
TECHNOLOGICAL  
UNIVERSITY  
SINGAPORE**

# Motivation

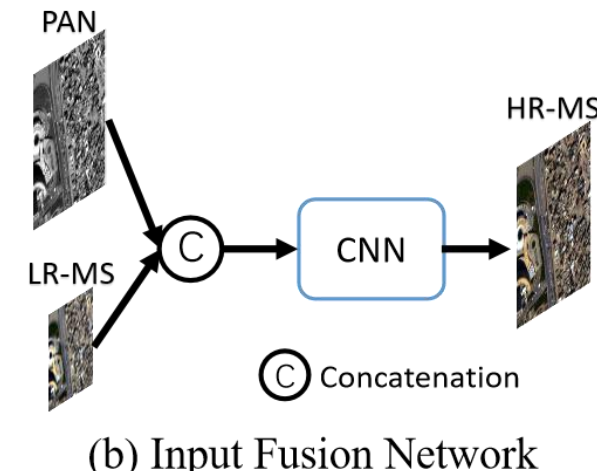
## Background:



- DL-based methods:



(a) Feature Fusion Network



(b) Input Fusion Network



# Motivation

## Motivation:

Model-driven CNN models:

The previous DL-based networks roughly stack the existing CNN frameworks, but they don't effectively utilize the spatial and spectral information of PAN and LRMS images, resulting in large redundancy in structural design.

Recently, some model-driven CNN models with clear physical meaning emerged. **The basic idea is to use prior knowledge to formulate optimization problems for computer vision tasks, then unfold the optimization algorithms and replace the steps in the algorithm with deep neural networks.**

- However, the optimization algorithms of model-based deep learning methods still require well-designed priors or assumptions. Additionally, the convergence of the optimization algorithms is not taken into account in the design of the unrolling networks.

## Our method:

- To address these problems, we propose a novel pan-sharpening approach called alternating reverse filtering network, which combines classical reverse filtering and deep learning. We formulate pan-sharpening as a reverse filtering process, thus avoiding the dependency on pre-defined priors or assumption. In addition, we tailor the classical reverse filtering in an alternating iteration manner for the pan-sharpening problem

# Methodology

## Model formulation:

- Inspired by classical reverse filtering, we propose alternating reverse filtering method to estimate HRMS by the more general multispectral image priors:

$$\begin{aligned}\mathbf{L} &= f(\mathbf{H}), \\ \mathbf{P} &= g(\mathbf{H}_I),\end{aligned}$$

### Reverse Filtering:

Filtering process can be described as  $\mathbf{y} = F(\mathbf{x})$ ,

When  $F(\cdot)$  is unknown, it's difficult to apply well-designed image priors to obtain the  $\mathbf{x}$ .

Reverse filtering can estimate  $\mathbf{x}$  without needing to compute  $F^{-1}(\cdot)$  and update restored images

$$\mathbf{x}^{k+1} = \mathbf{x}^k + \mathbf{y} - F(\mathbf{x}^k),$$

We tailor the classical reverse filtering in an alternating iteration manner for the pan-sharpening problem:

$$\left\{ \begin{array}{lcl} \mathbf{H}^{k+\frac{1}{2}} & = & \mathbf{H}^k + \hat{\mathbf{L}} - f(\mathbf{H}^k) \\ \tilde{\mathbf{H}}_I^k & = & \mathbf{H}_I^{k+\frac{1}{2}} \\ \tilde{\mathbf{H}}_I^{k+1} & = & \tilde{\mathbf{H}}_I^k + \mathbf{P} - g(\tilde{\mathbf{H}}_I^k) \\ \mathbf{H}^{k+1} & \Leftarrow & (\mathbf{H}_I^{k+\frac{1}{2}} \leftarrow \tilde{\mathbf{H}}_I^{k+1}), \end{array} \right.$$

# Methodology

## Model formulation:

- The forward process of alternating reverse filtering network can be described as Algorithm 1:

---

**Algorithm 1** Proposed algorithm.

**Input:** The upsampled low-resolution multispectral image  $\hat{\mathbf{L}}$ , panchromatic image  $\mathbf{P}$  and maximum iteration number  $K$ .

initial  $\mathbf{H}^0 = \hat{\mathbf{L}}$ ;

**for**  $k = 0, 1, 2, 3, \dots, K$  **do**

    compute  $\mathbf{H}^{k+\frac{1}{2}} = \mathbf{H}^k + \hat{\mathbf{L}} - f(\mathbf{H}^k)$ ;

    fetch the intensity component  $\tilde{\mathbf{H}}_I^k = \mathbf{H}_I^{k+\frac{1}{2}}$ ;

    compute  $\tilde{\mathbf{H}}_I^{k+1} = \tilde{\mathbf{H}}_I^k + \mathbf{P} - g(\tilde{\mathbf{H}}_I^k)$ ;

    replace the intensity component  $\mathbf{H}_I^{k+\frac{1}{2}} \leftarrow \tilde{\mathbf{H}}_I^{k+1}$  to get  $\mathbf{H}^{k+1}$ ;

**end for**

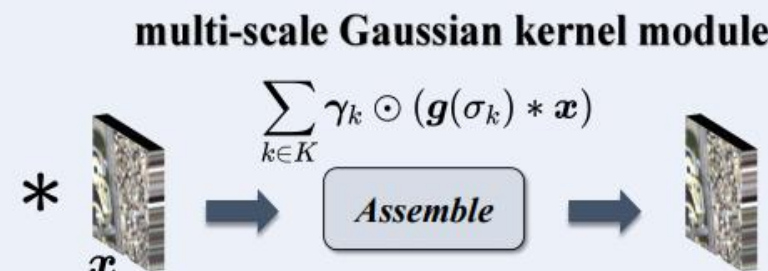
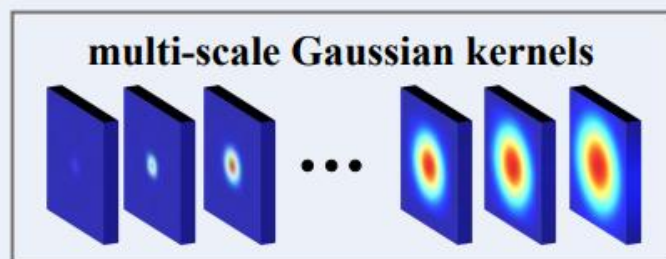
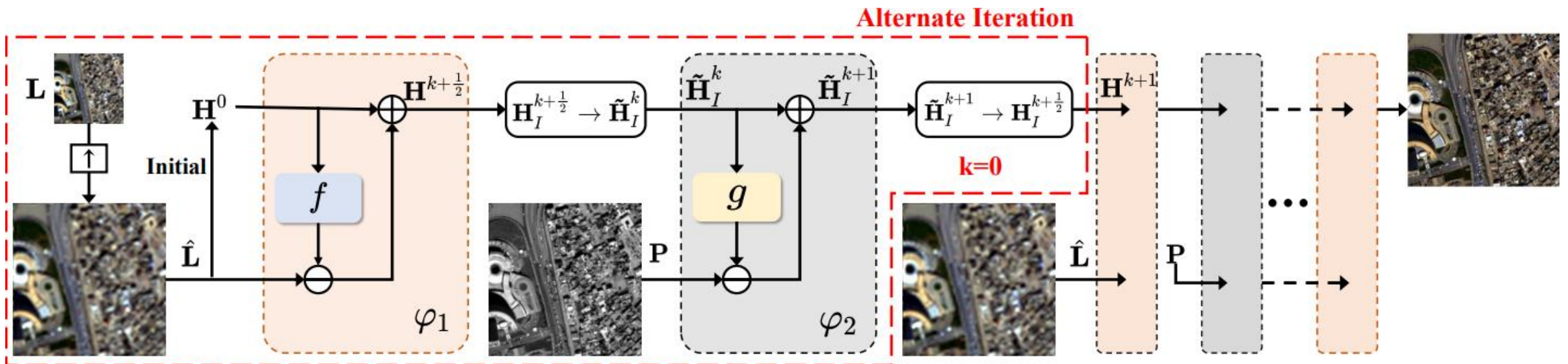
**Output:** fused high-resolution multispectral image  $\mathbf{H}^K$  and estimated intensity component  $\tilde{\mathbf{H}}_I^K$ .

---

# Methodology

## The detailed flowchart of our proposed method:

The overall architecture of alternating reverse filtering network:



$\oplus$  Element-wise addition

$\ominus$  Element-wise subtraction

$\uparrow$  BiCubic interpolation

$f$  Multi-scale Gaussian kernel module  
 $g$

# Experiments

## Quantitative comparison:

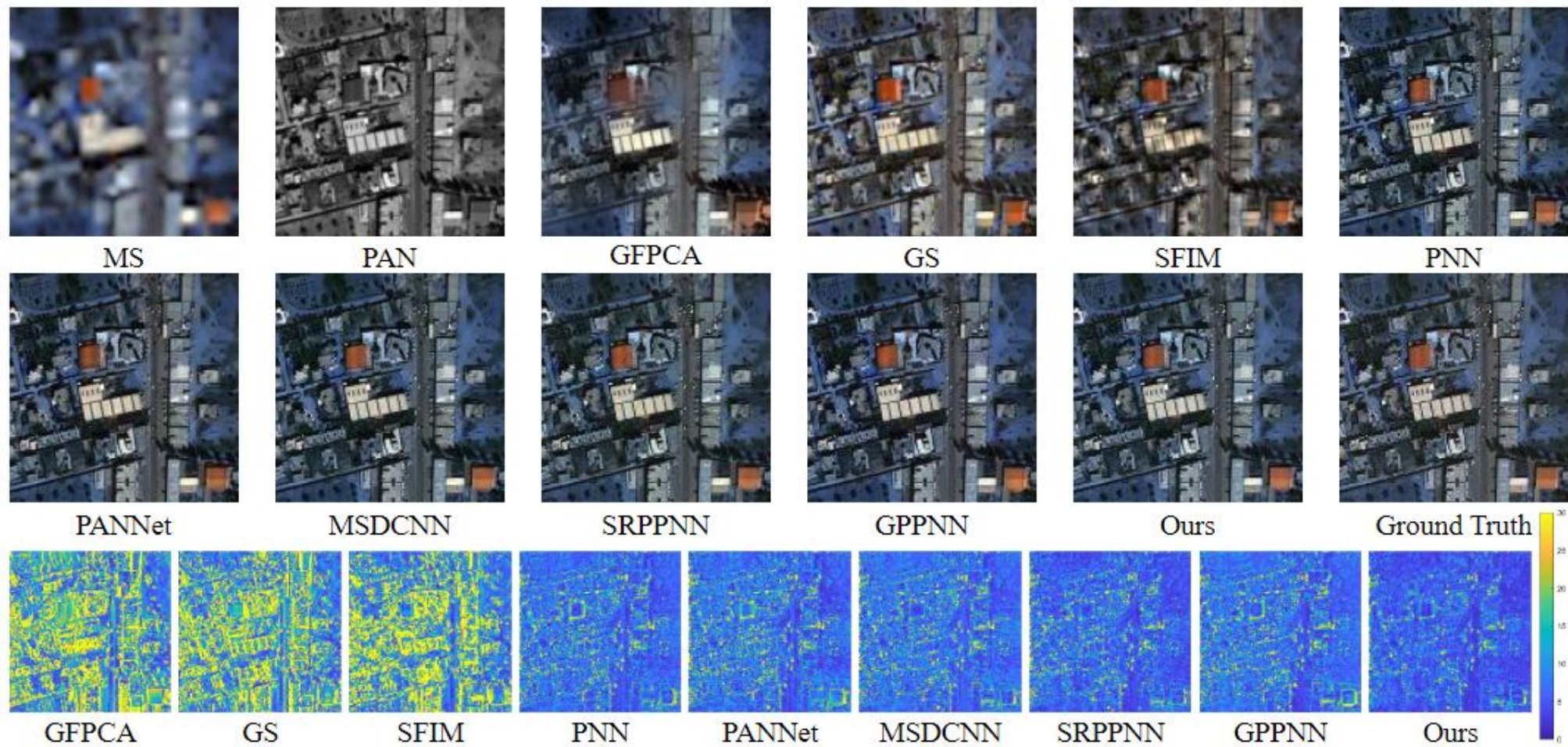
Table 1: Quantitative comparison with the state-of-the-art methods. The best results are highlighted by **bold**. The  $\uparrow$  or  $\downarrow$  indicates higher or lower values correspond to better results.

Method	WordView II				GaoFen2				WordView III			
	PSNR $\uparrow$	SSIM $\uparrow$	SAM $\downarrow$	ERGAS $\downarrow$	PSNR $\uparrow$	SSIM $\uparrow$	SAM $\downarrow$	ERGAS $\downarrow$	PSNR $\uparrow$	SSIM $\uparrow$	SAM $\downarrow$	ERGAS $\downarrow$
SFIM	34.1297	0.8975	0.0439	2.3449	36.9060	0.8882	0.0318	1.7398	21.8212	0.5457	0.1208	8.9730
Brovey	35.8646	0.9216	0.0403	1.8238	37.7974	0.9026	0.0218	1.3720	22.506	0.5466	0.1159	8.2331
GS	35.6376	0.9176	0.0423	1.8774	37.2260	0.9034	0.0309	1.6736	22.5608	0.5470	0.1217	8.2433
IHS	35.2962	0.9027	0.0461	2.0278	38.1754	0.9100	0.0243	1.5336	22.5579	0.5354	0.1266	8.3616
GFWPCA	34.5581	0.9038	0.0488	2.1411	37.9443	0.9204	0.0314	1.5604	22.3344	0.4826	0.1294	8.3964
PNN	40.7550	0.9624	0.0259	1.0646	43.1208	0.9704	0.0172	0.8528	29.9418	0.9121	0.0824	3.3206
PANNet	40.8176	0.9626	0.0257	1.0557	43.0659	0.9685	0.0178	0.8577	29.684	0.9072	0.0851	3.4263
MSDCNN	41.3355	0.9664	0.0242	0.9940	45.6874	0.9827	0.0135	0.6389	30.3038	0.9184	0.0782	3.1884
SRPPNN	41.4538	0.9679	0.0233	0.9899	47.1998	0.9877	0.0106	0.5586	30.4346	0.9202	0.0770	3.1553
GPPNN	41.1622	0.9684	0.0244	1.0315	44.2145	0.9815	0.0137	0.7361	30.1785	0.9175	0.0776	3.2596
Ours	<b>41.7587</b>	<b>0.9691</b>	<b>0.0229</b>	<b>0.9540</b>	<b>47.2238</b>	<b>0.9892</b>	<b>0.0102</b>	<b>0.5495</b>	<b>30.5425</b>	<b>0.9216</b>	<b>0.0768</b>	<b>3.1049</b>

# Experiments

## Qualitative comparison:

The qualitative results on WorldView-III datasets:



# Experiments

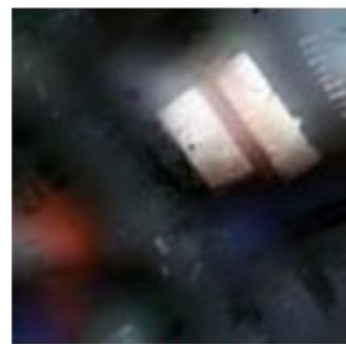
Visual comparisons of the fused HRMS image on a full resolution sample



Real LR MS



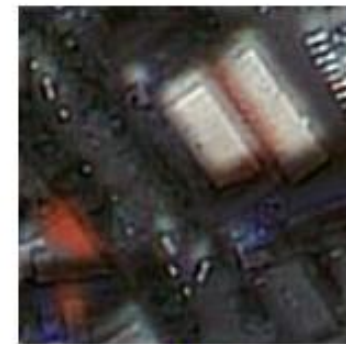
Brovey



GPCA



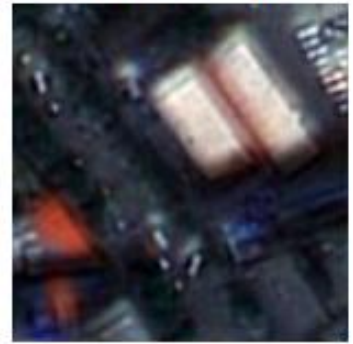
GS



SFIM



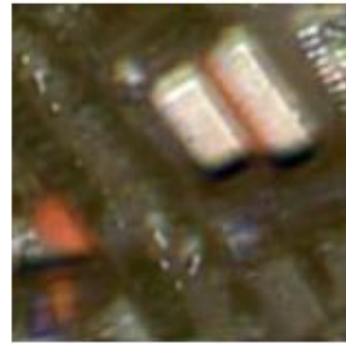
PNN



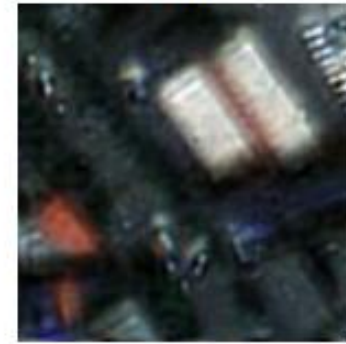
PANNNet



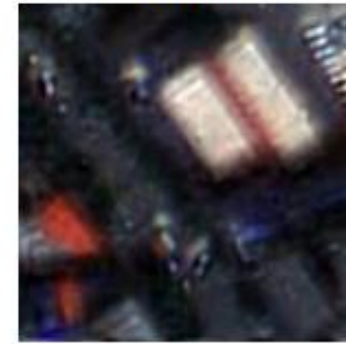
MSDCNN



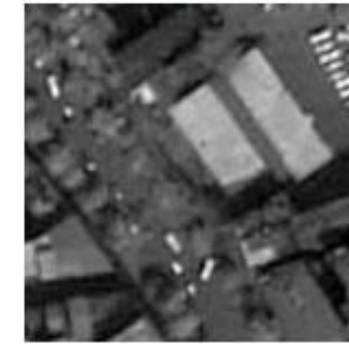
SRPPNN



GPPNN



Ours



PAN

# Experiments

## Ablation experiments:

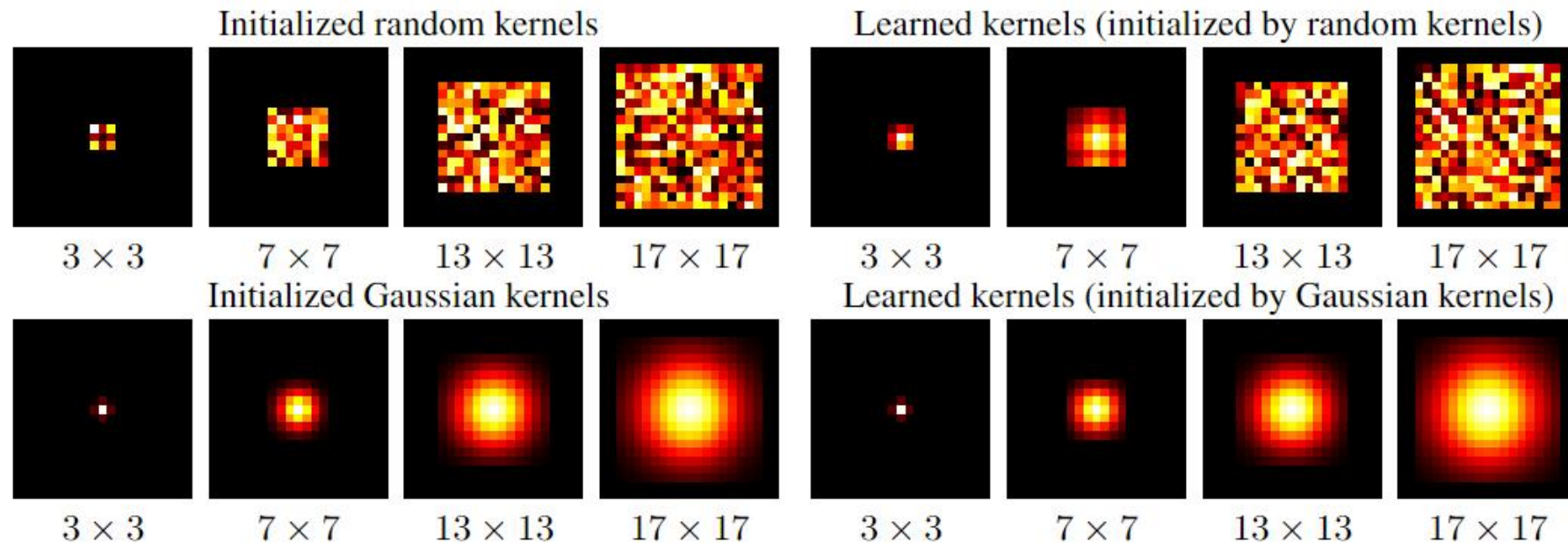


Table 4: Quantitative comparison of different initialization methods on the WorldView-II dataset.

Methods	PSNR↑	SSIM↑	SAM↓	ERGAS↓	SCC↑	Q↑	$D_\lambda \downarrow$	$D_S \downarrow$	QNR↑
(I)	40.3297	0.9601	0.0262	1.0672	0.9663	0.7310	0.0698	0.1277	0.8097
(II)	<b>41.7587</b>	<b>0.9691</b>	<b>0.0229</b>	<b>0.9540</b>	<b>0.9749</b>	<b>0.7731</b>	<b>0.0631</b>	<b>0.1184</b>	<b>0.8285</b>
(III)	40.4161	0.9612	0.0261	1.0668	0.9667	0.7316	0.0684	0.1275	0.8123



A large, semi-transparent graphic of a human brain in shades of blue and grey occupies the center-left of the slide. Overlaid on the right side of the brain is a dark blue circuit board with white lines representing data pathways. The background of the slide is a gradient from light blue at the top to dark blue at the bottom.

# Thanks for your attention!

